COUPLING BETWEEN RECTANGULAR PANEL MODES AND ACOUSTICAL MODES IN RECTANGULAR CAVITY+

Adnan D. Mohamed* **Saffa H. abdul – Rahman***
Hassan H. Mahdi** **Mahmood A. Hassan*****

Abstract

The response of structure to internal sound in an enclosure has received a considerable attention from designers because of the induced stresses in the structure from acoustic excitation. The main aim of this research was to investigate the modal interaction between structural modes and acoustical modes using different coupled configurations and evaluation of the response of the structure theoretically and experimentally. Another objective was to investigate the effect of damping, thickness, material properties, boundary condition on the radiation efficiency.
The analysis involved the prediction of energy transfer between acoustic and the structural systems employing the well known coupled oscillatory theory.

A system consists of a flexible rectangular (simply supported and simply clamped) panel, which forms one wall of rigid rectangular box, is analyzed analytically. The acoustic space is excited by a random source and the results of averaged radiation efficiency from the panel were predicted in different 1/3 octave frequency bands. Acceptable agreement between experimental and theoretical results is observed from the model of panel cavity.

The results of this work show that the radiation efficiency, increases with increasing the thickness of the panel, and decreases with increasing the damping of the structure and acoustic space. The results also show that the radiation efficiency of brittle material is higher than that of ductile material; it is observed that the boundary condition of the structure has a great effect on the radiation efficiency. The response of the simply clamped panel is higher than that of simply supported panel.

Keywords: **Coupling, acoustical modes, structural modes and rectangular cavity.**

المستخلص

استجابة الهيكل الى الصوت المتولد داخل جوف (أي فراغ هوائي) تعطي أهمية كبيرة من قبل المصممين وذلك بسبب ألاجهادات المتولدة في الهيكل نتيجة التهيج (ألاثارة) الصوتية. ان الهدف الرئيس من البحث هو دراسة الربط بين الاطوار

+ Received on 2/4/2007 , Accepted on 13/2/2008
* Asst. prof., University of technology
** Lecturer, Technical college – Baghdad
*** Asst. Lecturer, Alqadisya University

الهيكلية والاطوار الصوتية باستخدام أشكال ربط مختلفة وتقييم استجابة الهيكل نظريا وعمليا. الهدف الاخر من البحث كان دراسة تاثير التخميد، السمك، خواص المادة، الشروط الحدية على كفاءة الاشعاع.

يتضمن التحليل دراسة (تكهن) الطاقة المنتقلة بين انظمة صوتية-هيكلية-مترابطات والخاضعة الى مايعرف بنظرية الاثارة المترابطة (Coupled oscillator theory) (الترابط الترددي). يتكون النظام من لوح مرن (Simply supported plate) الذي يكون احد جدران الصندوق المكعب الشكل والذي حل عدديا. اثير الفراغ الصوتي عشوائيا وتمت دراسة معدل طاقة الاشعاع للوح باستخدام حزم ترددية (1/3 octave bands) مختلفة.

نتائج هذا العمل بينت بان كفاءة الاشعاع تزداد مع زيادة سمك اللوح وتقل بزيادة تخميد الهيكل والفراغ الصوتي. وبينت النتائج أيضا بان كفاءة الاشعاع للمواد الهشة هي اعلى من المواد المطيلية بالاضافة الى ذلك، لوحظ بان الظروف الحدية للهيكل لها تاثير كبير على كفاءة الاشعاع. وأخيرا لوحظ ان استجابة أل (Simply camped panel) تكون أكبر من أل (simply supported panel).

Introduction

Acoustic may be defined as the generation, transmission and reception of energy in the form of vibrational waves in matter. As the atoms or molecules of a fluid or solid are displaced from their normal configuration, an internal elastic restoring force arises.
The physical manifestation of sound is a time – dependent pressure fluctuation around the static pressure in a compressible fluid, such as air or water. The fluctuation pressure on the surface of the structure constitutes the radiation loading. To obtain the resultant load, this distributed loading is combined with the prescribed forces that are the prime sources of the structural vibrations. Because of the low density of air compared to structural materials, radiation loading exerted by the atmosphere is generally small enough to have a negligible effect on the structural vibration. Radiation loading modifies the motion of a structural vibrating in the atmosphere only under circumstances. Thus, in most situations, the dynamic response of a structure in the atmosphere, excited by prescribed driving forces, can be determined as though the structure were vibrating in a vacuum. Subsequently the uncoupled acoustical problem of evaluation the pressure field generated by a velocity distribution prescribed over the boundary of the acoustic medium can be solved independently.

In order to determine the direction of this research, a number of published papers were reviewed. Fahy et al. [1], proposed the input power modulation technique proposed as an alternative to the widely used steady-state power injection method for the in-situ determination of dissipation and coupling loss factor of subsystem selected for a Statistical Energy Analysis (SEA) model of a physical system. There is no requirement of measure input power and, in principal response measurement are made only one point on each subsystem. Theory is developed for a two subsystem model.

James et al. [2] presented the result of an experimental application of the technique to two plates coupled by a variable number of straps and two rooms coupled by an aperture. Similar value of the coupling strength indicator (Cs) to those theoretically evaluated is observed.

Frendi et al. [3] studied the problem of coupling between panel vibrations and near and far field acoustic radiation. Two models have been used to solve this structural - acoustic interaction problem. The prediction given by these two modes are in a good agreement, but the computational time needed for the “fully coupled model” is 60 times longer than that for “the decoupled model”.

Zhozo et al. [4], developed the active noise control, which is effective for low frequency band, when high control performance would be achieved in the enclosed cavity, it is necessary to measure the sound pressure at many measuring points in the cavity, but it is hard to set many sensors in the cavity because of the lack of space or cost problem.

Yoshida [5], studied the vibration responses of spacecraft equipment structures, especially lightweight rigid panel excited by a low frequency acoustical noise field. The experimental results of the acceleration responses or the panel in the random sound field were found to agree with the simulation results of this proposed calculation method, and the simulation results of the usual frequency response method contain a high degree of error compared with the result of the new method.

Laesia [6] presented a method to estimate the response of an aerospace structure excited by the acoustical loads produced during a rocket launch (high acceleration level achieved). This method is based on Kirchhoff integral formulation of the Helmholtz equation for the pressure field. Comparisons of the present method with various experimental data and other theories show the efficiency and accuracy of this method for any support condition of the plate and validity of the present procedure for the value of the frequency of excitation that appears in an acoustical test performed in a large reverberant chamber.

Yan et al [7] investigated the noise problem in an aluminum motor vessel. Various control measures for reducing the deck noise are discussed and preliminary results on deck noise measurements of the modified vessel are presented.

Kim and Brennan [8] concluded that the analytical and experimental investigation which compares the feed forward control of harmonic and random sound transmission into an acoustic cavity. A rectangular enclosure is considered. It was shown that the configuration of both acoustic and structural actuators is desirable for the active control of both harmonic and random sound transmission into a coupled structural-acoustic system whose response is governed by plate and cavity-controlled modes.

Guoyong et al [9] presented an analytical investigation into the active control of sound transmission into a structural-acoustic coupled system. An enclosure with four acoustically rigid walls and two simply supported flexible plates is considered. One of the two plates through which a harmonic sound wave is transmitted into the enclosure, is called as incident plate here, and the other as the receiving plate. Based on a fully coupled vibro-acoustic model, six different control strategies, i.e. control arrangements, are compared and discussed. They are: (a) incident plate control using distributed piezoelectric actuators, (b) applying acoustic control source in the cavity (called as cavity control), (c) receiving plate control using distributed piezoelectric actuators, (d) hybrid control combining incident plate control and cavity control, (e) hybrid control combining receiving plate control and cavity control, (f) simultaneous use of both incident plate actuator and receiving plate actuator. The analytical results show that hybrid control combining incident plate control and cavity control and simultaneous use of both incident plate actuator and receiving plate actuator are desirable configurations for the active control of sound transmission into a structural-acoustic coupled system surrounded by two flexible plates in terms of the acoustic potential energy inside the enclosure.

Theoretical aspect

A plate is a two dimensional sheet of elastic material, which lies in a plane. Plates, unlike membranes, possess bending rigidity as a result of their thickness and elasticity of the plate material. During transverse vibration, plates deform primarily by flexing perpendicular to their own plane.

The sound in a room consists of that coming directly from the source plus sound reflected or scattered by the walls and by objects in the room. Sound having undergone one or more reflections is called reverberant sound because it corresponds for an impulsive source to a series of echoes. If the direct wave predominates almost everywhere, the room is anechoic; rooms so designed are anechoic chambers. A reverberation chamber is a room designed so that the reverberant field is the dominant one.

In this study a case of coupling between structure (flat plate) and an excited acoustic field (rectangular room) is analyzed. Results for radiation efficiency (response) are demonstrated. The analysis may be treated as a sequel to that of Fahy [10], using its basic theory.

Coupling between structure and fluid volume

The basic of the following analysis is the coupled oscillator theory [11] and [12]. The differential equations of forced motion of two coupled sets of oscillators represented structural modes and acoustic modes are written (for coupled mode pairs) as [12] and [13];

$$\ddot{S}_m + \beta_m \dot{S}_m + \omega_m{}^2 S_m + \sum_r B_{mr} \dot{q}_r = F_m \qquad (1a)$$

$$\ddot{q}_r + \beta_r \dot{q}_r + \omega_r{}^2 q_r - \sum_m B_{mr} \dot{S}_m = G_r \qquad (1b)$$

Where

$$\ddot{S}_m = \sqrt{\varepsilon_m S'_m} \quad ; \quad q_r = \sqrt{\frac{\rho V \varepsilon_r}{M C_o^2}} q'_r \quad ; \varepsilon_m = M^{-1} \int_s \phi_m^2(x) m''(x) dx \quad and \quad \varepsilon_r = v^{-1} \int_v \psi_r^2(r) dr$$

If the coupling terms (last terms in equation (1a) and (1b)) are incorporated into the forcing terms, equations (1a) and (1b) become

$$\ddot{S}_m + \beta_m \dot{S}_m + \omega_m^2 S_m + B_{mr} \dot{q}_r = F_m - \sum_{k \neq r} B_{km} \dot{q}_k = F'_m \qquad (2a)$$

$$\ddot{q}_r + \beta_r \dot{q}_r + \omega_r^2 q_r - B_{mr} \dot{S}_m = G_r + \sum_{n \neq m} B_{nr} \dot{S}_n = G'_r \qquad (2b)$$

With the assumption that F'_m and G'_r are independent and “white”, equations (2) now represent the coupled motion of only two oscillations which Lyon and Maidanik [11] wrote the power flow per unit mass from the mth to the rth mode as

$$j_{mr} = g_{mr} (\theta'_m - \theta'_r) \qquad (3)$$

With further assumption that the parameter (B_{mr} / β_r) and (B_{mr} / β_m) are very small (weak coupling assumption), the coupling constant g_{mr} is then derived as

$$g_{mr} = \frac{B_{mr}^2 (\beta_m \omega_r^2 + \beta_r \omega_m^2)}{(\omega_m^2 - \omega_r^2)^2 + (\beta_m + \beta_r)(\beta_m \omega_r^2 + \beta_r \omega_m^2)} \qquad (4)$$

Where

$$B_{mr} = \left[\frac{C_o^2 \rho}{V \varepsilon_r \varepsilon_m M} \right]^{1/2} \int_S \psi_r(x) \phi_m(x) dx \qquad (5)$$

The important feature of equation (4) is the strong sensitivity of the denominator to the difference between the structural and acoustic modes natural frequencies, which enable the following first order approximation [10].

$$g_{mr} \approx B_{mr}^2 (\beta_m + \beta_r)^{-1} \quad : |\omega_m - \omega_r| \prec \frac{1}{2}(\beta_m + \beta_r) \qquad (6a)$$

$$g_{mr} \approx 0 \quad : |\omega_m - \omega_r| \succ \frac{1}{2}(\beta_m + \beta_r) \qquad (6b)$$

The conditions of equation (6) are considered in the analysis of the present work as a criterion to separate the significant acoustic-structure mode pairs, which are referred to as having "proximate mode coupling".

Panel – Box system

The coupled system analyzed consists of a thin, steel, elastic, rectangular, simply supported panel of a uniform thickness and density. The panel forms one complete wall of an otherwise rigid rectangular box containing air with dimensions of (0.82m x 0.65m x 3mm). The box had the dimensions of (0.82m x 0.65m x 0.6m). The configuration of the system is shown in fig (1). The panel and the fluid in the box represent the coupled multi-mode systems.

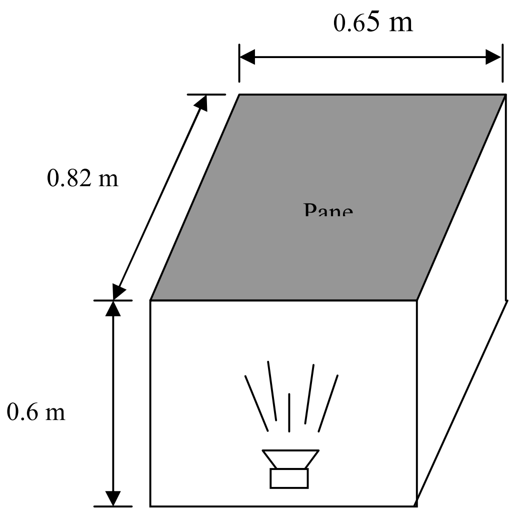

Fig (1) Panel box model

The eigenfunctions of the structural displacement is given by [10].

$$\phi_m(x,y) = \sin\left(\frac{m\pi x}{a}\right) \sin\left(\frac{n\pi y}{b}\right) \qquad (7)$$

The eigenfunctions of the acoustic velocity potential is given by [10].

$$\psi_r(x,y,z) = \cos\left(\frac{p\pi x}{a}\right) \cos\left(\frac{q\pi y}{b}\right) \cos\left(\frac{r\pi z}{c}\right) \qquad (8)$$

The substitution of these eigenfunctions into equation (5) for B_{mr} gives

$$B_{mr} = K(-1)^r \left[\frac{ma}{p^2\pi} \left\{ \frac{(-1)^m(-1)^p - 1}{1-(m/p)^2} \right\} \right] \left[\frac{nb}{q^2\pi} \left\{ \frac{(-1)^n(-1)^q - 1}{1-(n/q)^2} \right\} \right] : m \neq p; n \neq q \tag{9}$$

$B_{mr} = 0$ for (m+p) even
or (n+q) even

Where

$$K = \left(\frac{c_o^2 p}{V\varepsilon_r \varepsilon_m M} \right)^{1/2}$$

The natural frequencies of acoustic mode ω_r and structural mode ω_m are calculated as [14], [15] and [16].

$$\omega_r = k_r C_o \tag{10}$$

$$\omega_m = k_p C_b \tag{11}$$

$$k_r = \sqrt{\left(\frac{p\pi}{a}\right)^2 + \left(\frac{q\pi}{b}\right)^2 + \left(\frac{r\pi}{c}\right)^2}$$

k_p for boundary condition (SS-SS-SS-SS) rectangular plate it is given by

$$k_p = \sqrt{\left(\frac{m\pi}{a}\right)^2 + \left(\frac{n\pi}{b}\right)^2}$$

And for boundary condition (SS-C-SS-C) rectangular plate [16]

$$k_p = \sqrt{\left(\frac{m\pi}{a}\right)^2 + \left(\frac{n\pi + 0.5\pi}{b}\right)^2}$$

C_b is given by $C_b^2 = \dfrac{D}{\rho_s h}\left\{ \left(\dfrac{m\pi}{a}\right)^2 + \left(\dfrac{n\pi}{b}\right)^2 \right\}$

And D is given by $D = \dfrac{Eh^3}{12(1-\nu^2)}$

Because of the flexural waves and dispersive, there is a unique frequency for every uniform elastic panel, which free waves travel with the same speed C_b , as sound waves in the adjacent fluid. These frequency is called the critical frequency f_c and is given by

$$f_c = \frac{C_o^2}{1.8hC_L} \tag{12}$$

Where $C_L = \sqrt{\dfrac{E}{\rho}}$

The critical frequency for the Aluminum panel (3 mm thickness) of the present model is about (4475) Hz from equation (12). The radiation resistance (R_{rad}) is given by

$$R_{rad} = \left(\frac{M}{N_s(\omega)} \right) \sum_{r,m} g_{mr} \tag{13}$$

Equation (13) is based on the assumption that the structural mode in the frequency band $\Delta\omega$ is coupled to all acoustic modes that exist in the frequency band.

The coupling loss factor (η_{SA}) between a structure and acoustic field is most simply expressed by average radiation resistance of structure (R_{rad}) interacting with an infinite space (diffuse sound field). It is written as [17];

$$\eta_{SA} = \frac{R_{rad}}{\omega M}$$

The radiation efficiency of the panel in the given frequency band of interest is given by

$$\sigma = \frac{R_{rad}}{\rho c_o ab} \qquad (14)$$

Figures (11) to (20) show plotted radiation efficiency for various thicknesses of plates.

Computer program

A computer program written in FORTRAN language is constructed to follow the analyses described in the previous section for the panel-box model specified earlier.

The program executes the following steps:

(a) The calculation of all possible natural frequencies of the panel modes (ω_m) and the box acoustic modes (ω_r) in the different 1/3 octave frequency bands of interest ranging from (0 to 6300) Hz center frequency.
(b) The assumption of a value for the parameter ($\beta_r+\beta_m$) which is the sum of the half-power bandwidths (model damping coefficients) of the structural and acoustic modes. Note that:

$$\beta_m = \omega_m \eta_m \quad and \quad \beta_r = \omega_r \eta_r$$

The following steps used to calculate the model radiation efficiency:

(a) Calculation of all possible natural frequencies of the acoustic modes (ω_r) and panel modes (ω_m) in the frequency band of interest using equation (10) and (11).
(b) Assuming a value for the parameter ($\beta_r+\beta_m$) which is the sum of the half-power bandwidths (model damping coefficients) of the structure and acoustic modes.
(c) Selection of all acoustic modes having natural frequencies sufficiently close to each natural frequency of the panel mode and obeying the frequency approximately condition of equation (6a) in the frequency band of analysis.
(d) Calculation of the coupling (B_{mr}) using equation (9) for each mode pair that was located in step (c) above.
(e) Calculation of the coupling constant (g_{mr}) for each mode pair according to equation (4).
(f) Calculation of radiation resistance (R_{rad}), using equation (13) and the radiation efficiency of the panel, in the given frequency band of interest, by using equation (14).

Steps (a-f) above are carried out, for different thickness (15, 25, 40 and 60 mm) and also in different 1/3 octave frequency bands. The results are plotted in figures (11) to (22).

Experimental investigation

In order to support the theoretical work illustrated in section (3) and to assess the degree of accuracy required in both theoretical approaches measurements were made on the response of a rectangular panel to an acoustic excitation in rectangular cavity. The response was on the form of radiation efficiency.

Test rig

The main purpose of designing a rig was to enable the frequency response test on a simple rectangular room to be performed in order to calculate the radiation efficiency.

Fig (2) shows the general assembly of the test rig. It consists of a rectangular panel of dimensions (0.81m × 0.65m) made of aluminum or glass of different thickness which is supported so as to form one wall of a rectangular box of dimensions (0.81m × 0.65m × 0.6m). The edges were bolted to a very light channel section of low rotational and high shear stiffness (simply supported). The other walls were those of a 1.25 mm thick steel rectangular tank which was surrounded by 10 cm of sand in an outer wooden box. A power of (75 W) acoustic random noise was produced in the tank by internal generator of dual channel signal analyzer type B&K (2034) and power amplifier type B&K (2706) and two loudspeakers. Five accelerometers type B&K (4391) of a mass of 16 grams were used in the measurements. The panel radiation efficiency was measured directly by means of off-center point excitation with a vibration generator, (loudspeaker excitation).

In the same system only replace the loudspeaker by the mini shaker type B&K (4810) and used force transducer to measure damping ratio of panel from frequency response function magnitude.

3.2 <u>Instrumentations</u>

The experimental set-up used in the measurements of mean square velocity of the panel due to the indirect random excitation of the acoustic cavity is shown in fig (3).

The set-up used for damping measurements is illustrated in fig (4). Two configurations used for this test as shown in fig (5a) and fig (5b) for point and transfer methods respectively.

The following instrumentations were used to perform the experimental investigation [18];

(a) Dual channel signal analyzer type B&K 2034.
(b) Power amplifier type B&K 2706.
(c) Mini shaker type B&K 4810.
(d) Charge amplifier type B&K 2635.
(e) Force transducers type B&K 8200.
(f) Piezoelectric accelerometer type B&K 4391.

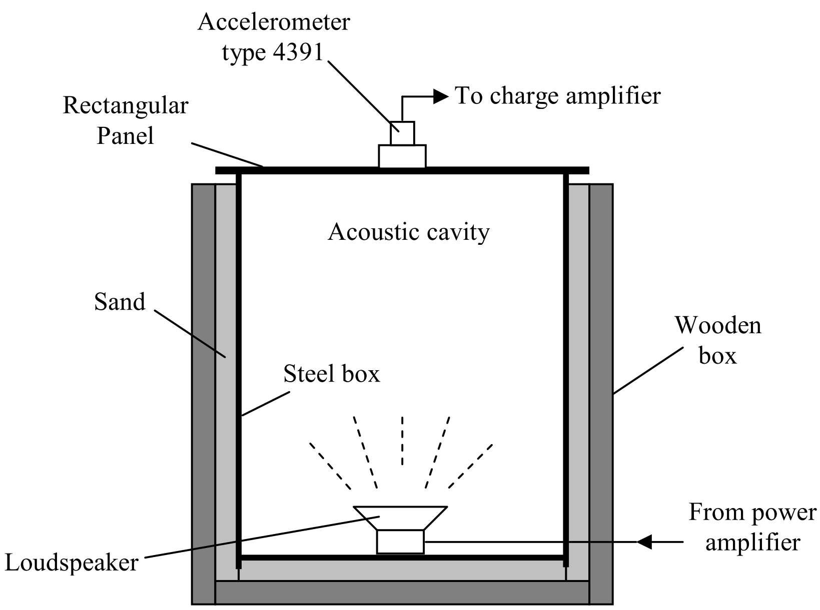

Fig (2) Test rig

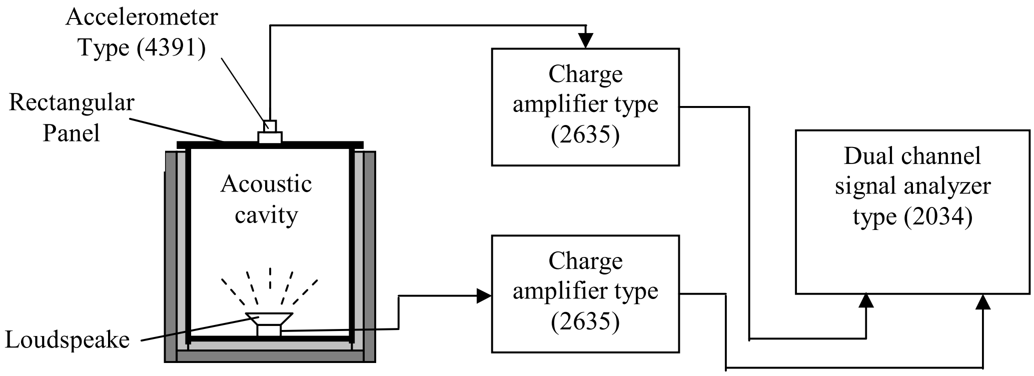

Fig (3) Wiring diagram of the general instrumentation for the test rig

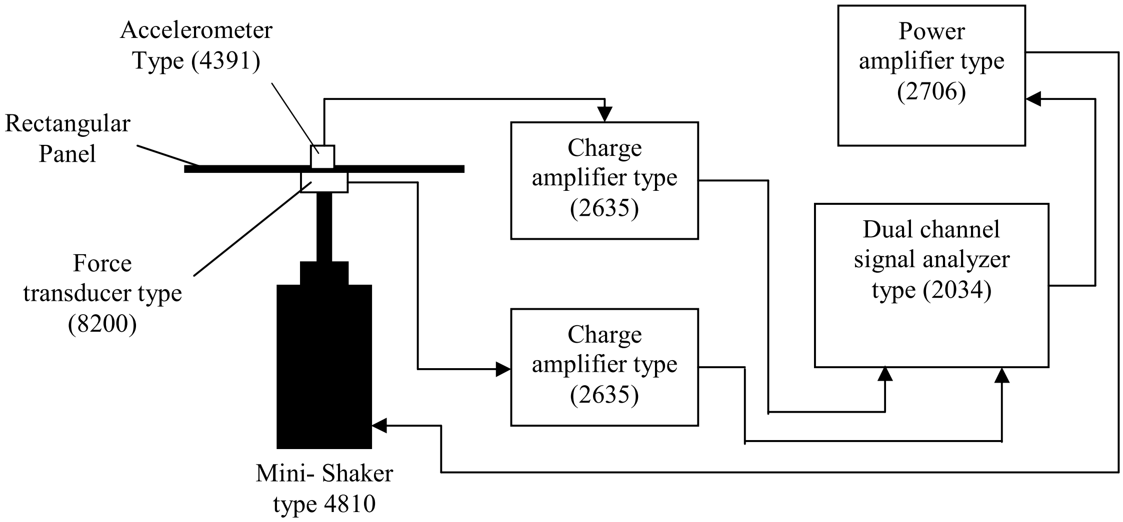

Fig (4) Wiring diagram of the instrumentation for the damping measurements

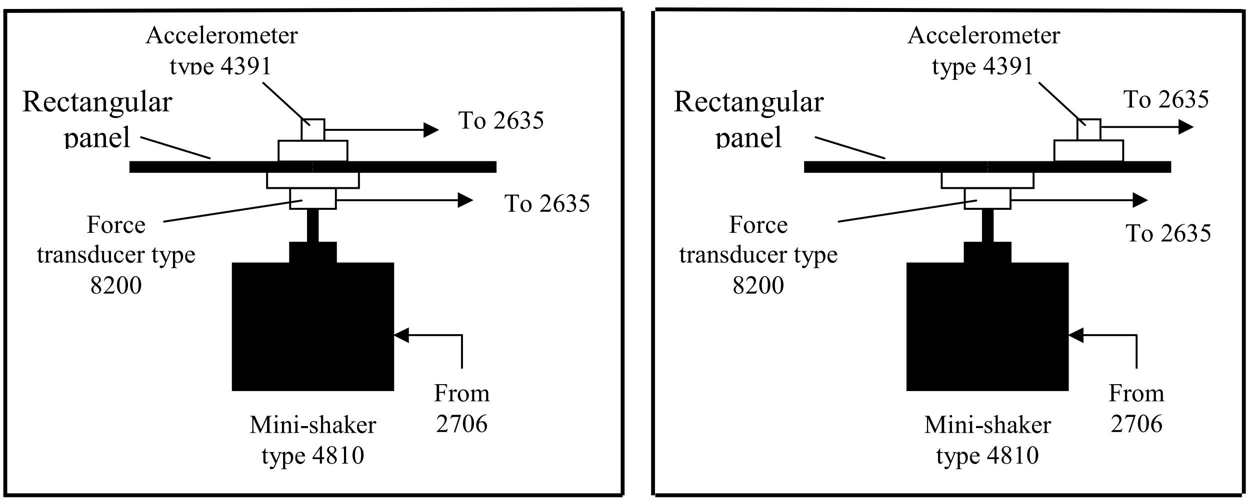

(a) (b)

Fig (5) Experimental configuration for damping measurements using
(a) Point frequency response function.
(b) Transfer frequency response function.

Damping measurements

The dissipation loss factor (η) of the panel was measured using the well known half power bandwidth method. The shaker at a given point on panel excites the panel. A band of random signal drives the shaker from the signal generator after being amplified by the power amplifier. And the accelerometers are fed to the spectrum analyzer through the charge amplifier. Results of frequency response in the form of dynamic compliance $\left(\frac{displacement}{force}\right)$ are demonstrated on the screen of the analyzer. If f_o represent the value of the selected resonance frequency of the frequency response, and Δf_{3dB} is the half power points (3dB down) of f_o (fig (6)), then the quality factor Q can be calculated as:

$$Q = \frac{f_o}{\Delta f_{3dB}}$$

and dissipation loss factor (η) can be found as:

$$\eta = \frac{1}{Q}$$

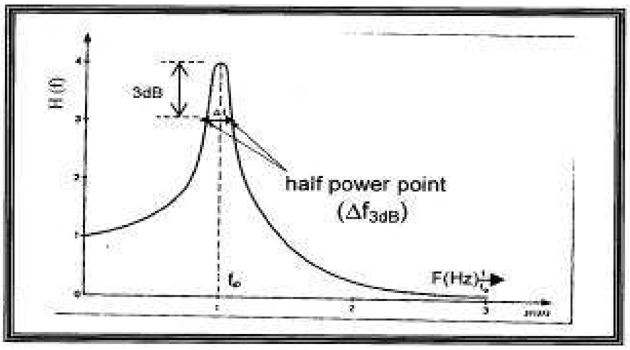

Fig (6) Resonance curve with the indication of the half power point [19]

Two configurations for the experimental set-up used for measurements of damping are shown in fig (5a) and fig (5b).

(1) Point frequency response function (point compliance) in which the force and responses at the same point fig (5a) results for f_o and Δf_{3dB} are recorded for different peaks of frequency response function and the average were calculated. This procedure is repeated at different locations on the panel. The average value of dissipation loss factor is found to be (η = 0.0146).

(2) Transfer frequency response function (transfer compliance) in which the force and response are at different points. The procedure above are repeated for this configuration and the average value of dissipation loss factor is found to be (η = 0.013) which is not in big difference from the previous configuration.

Typical curves of frequency response functions are shown in fig (7) and fig (8).

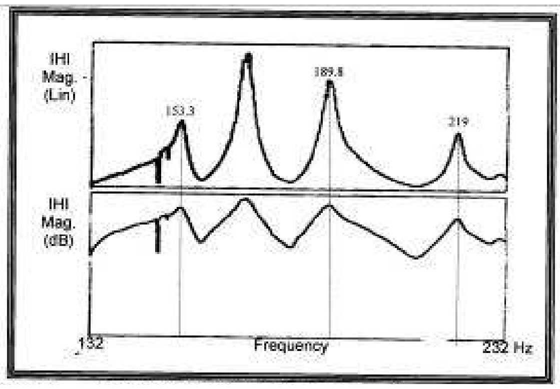

Fig (7) Damping measurement using point frequency response

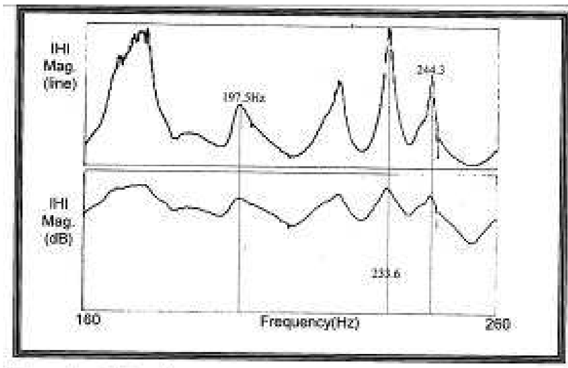

Fig (8) Damping measurement using transfer frequency response

Velocity measurements

This part of experimental work is performed using the experimental set-up shown in fig (3). The procedure is summarized as follows:

(1) A random, white noise, band-limiting signal is fed to the loudspeaker via the power amplifier. The loudspeaker is used to excite the system as an acoustic source. The bandwidth of the excitation is chosen to the standard 1/3 octave frequency bands.

(2) An accelerometer is attached to the panel for monitoring the response to the acoustic excitation in the form local velocity. Results of average mean square velocity $\left(\overline{V}^2\right)$ are calculated over the selected frequency bands.

(3) The radiation efficiency is defined as [20]

$$\sigma_{rad} = \frac{E_{rad}}{\rho_o CS\left(\overline{V}^2\right)}$$

Where E_{rad} is calculated from the source specifications. The measurement and the steps above are repeated for different 1/3 octave frequency bands.

(4) Results of radiation efficiency were compared with those obtained from theoretical predictions and are shown for different 1/3 octave bands fig (9) and

(5) fig (10).

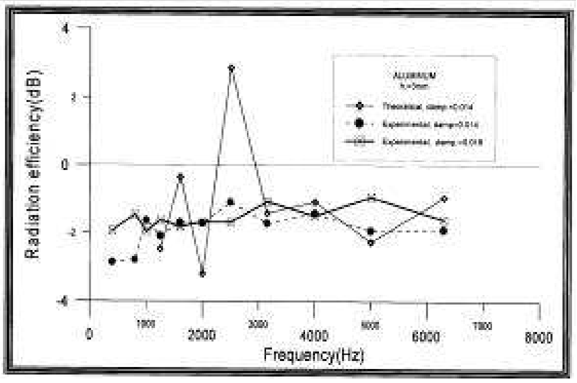

Fig (9) Theoretical and experimental radiation efficiency of 3 mm simply supported aluminum panel (1/3 octave band averages)

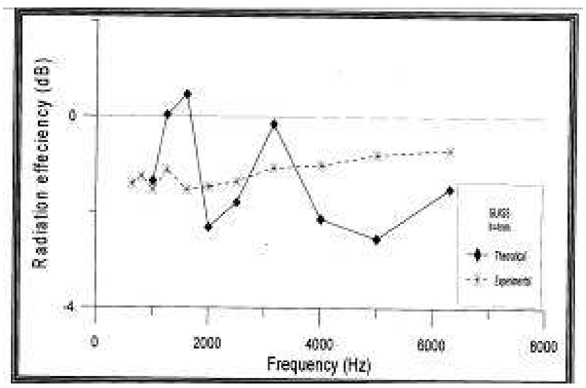

Fig (10) Theoretical and experimental radiation efficiency of 4 mm simply supported glass panel (1/3 octave band averages)

The main purpose of this section is to illustrate and discuss some of the results obtained from tests on the experimental rig shown in fig (2), and from execution of the computer program produced results for the theoretical investigation of the radiation efficiency, relating to the rectangular room.

Panel – cavity coupling (theoretical investigations)

Fig (11) and table (1) shows the effect of damping of the total system $(Y = \beta_m + \beta_r)$ on the computed results of radiation efficiency of (2 mm) aluminum panel with all four edges simply supported (S-S-S-S). The results are plotted for different 1/3 octave frequency bands. An obvious finding is observed here. As $(\beta_m + \beta_r)$ increases the response (radiation efficiency) decreases. This is because of increasing the damping effect, which increases the amount of energy dissipated in the panel. Another main finding observed is that as the frequency increases the value of radiation efficiency increases and approaching the value of 0 dB which corresponds to radiation from an infinite panel which is the ideal case. The main reason for this trend of the curve is that because of the increasing number of acoustic-structural mode pairs as the center frequency of the bands increases. This behavior of the results is compatible with Fahy [10].

Figs (12), (13), (14) and table (1) are the results of similar predictions but for plate thicknesses of 3, 4 and 5 mm respectively. They demonstrate the same trend of fig (11) but also show that increasing the thickness gives higher values for the radiation efficiency. This behavior may be because as the thickness increases the modal density (number of modes per unite frequency interval) increase which means that the number of active working mode pairs increases. Also, the low frequency results of radiation efficiency is considered to be poor estimates of the response because of the scatter behavior originated from the low number of acoustic-structural mode pairs.

Figs (15) to (18) and table (2) are similar to those discussed above except that different material (glass) is chosen for the panel. The aim was to study the effect of material properties on the response of the panel. Generally, the figures show that the radiation efficiency increases as the thickness of panel increase, while the response decreases as the value of $(\beta_m + \beta_r)$ increases. The difference between this set of figures and the previous set is that the radiation efficiency of the aluminum panel is less than that of glass panel especially at high frequencies.

Fig (19) and fig (20) summarized the effect of thickness of panel on the results for a given value of damping and for aluminum and glass with four edges simply supported. Increasing the thickness, results in an increased value of radiation efficiency.

Figs (21), (22) and table (3) summarized the effect of boundary conditions on the values of radiation efficiency. Higher values of radiation efficiency are reported for the clamped panel especially at high frequency region for both aluminum and glass panels. High frequency region is more important than the low frequency range in the comparison because the high frequency region is characterized by the high number of active mode pairs which is the ideal case in comparison

.

<u>Panel – cavity coupling (experimental investigations)</u>

It is observed from fig (9) for aluminum and fig (10) for glass panel that there is an acceptable agreement with some difference between the measured and calculated radiation efficiency within the frequency range 3000 Hz to about 6300 Hz. However, this difference

increases approximately up to 34% and 46% for the frequency range below 3000 Hz respectively. The differences were possibly due to modal averaging.
Figs (7) and (8) show typical graphs of point and transfer frequency response functions that are used in the measurements of dissipation loss factor of the aluminum panel. It is clear that there is a small difference in the measured dissipation loss factor of about 11% between the point and the transfer frequency response function.

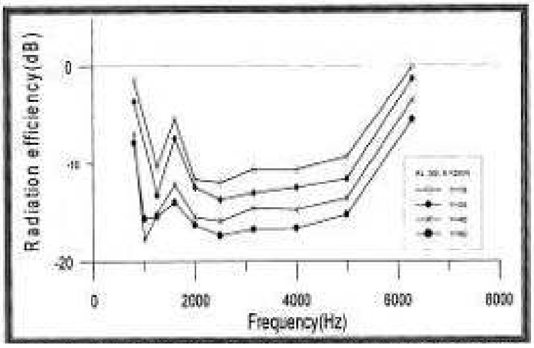

Fig (11) Radiation efficiency of 2 mm simply supported aluminum panel (1/3 octave band averages)

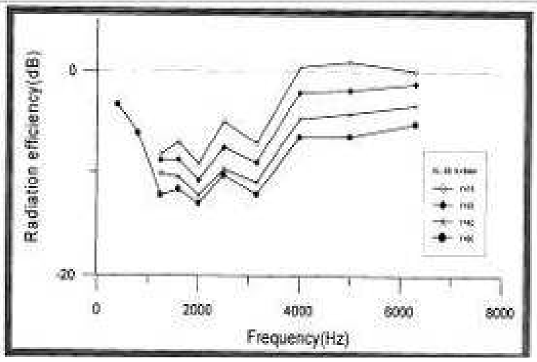

Fig (12) Radiation efficiency of 3 mm simply supported aluminum panel (1/3 octave band

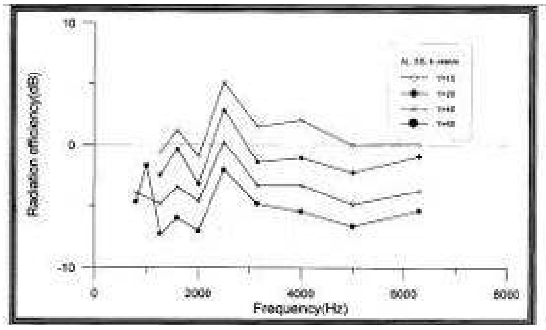

Fig (13) Radiation efficiency of 4 mm simply supported aluminum panel (1/3 octave band

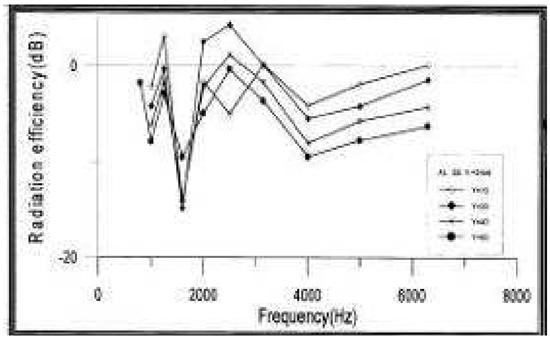

Fig (14) Radiation efficiency of 5 mm simply supported aluminum panel (1/3 octave band averages)

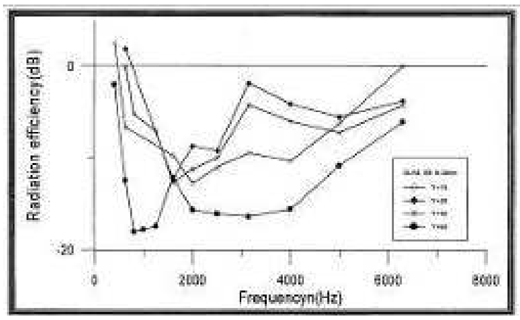

Fig (15) Radiation efficiency of 2 mm simply supported glass panel (1/3 octave band averages)

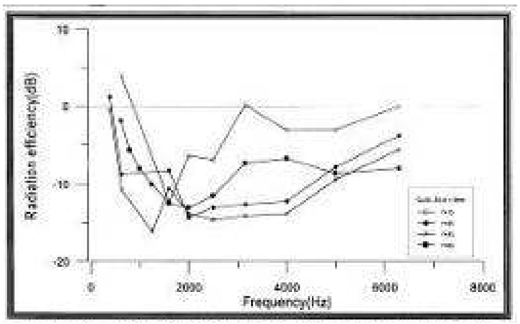

Fig (16) Radiation efficiency of 3 mm simply supported glass panel (1/3 octave band averages)

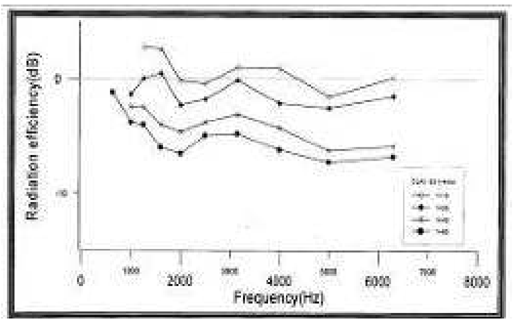

Fig (17) Radiation efficiency of 4 mm simply supported glass panel (1/3 octave band averages)

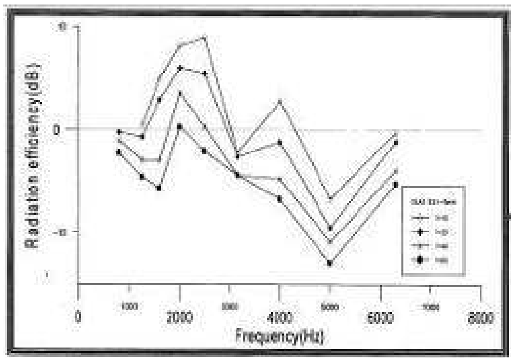

Fig (18) Radiation efficiency of 5 mm simply supported glass panel (1/3 octave band averages)

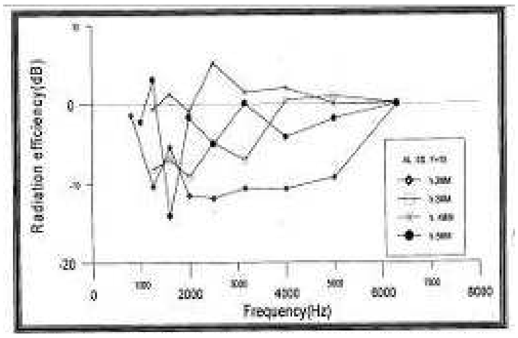

Fig (19) Effect of thickness on radiation efficiency of simply supported aluminum panel (1/3 octave

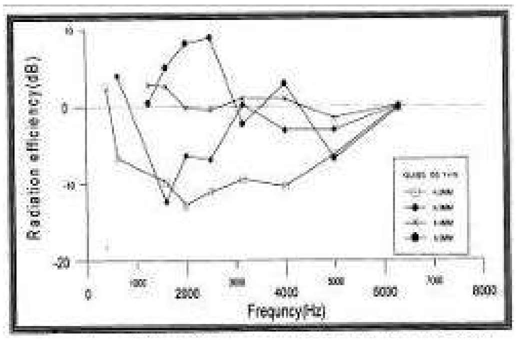

Fig (20) Effect of thickness on radiation efficiency of simply supported glass panel (1/3 octave band averages)

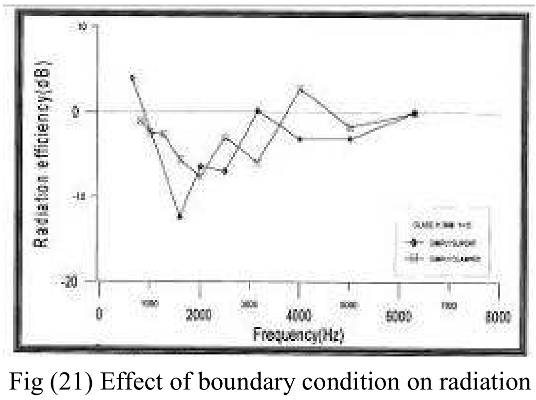

Fig (21) Effect of boundary condition on radiation efficiency of simply supported glass panel (1/3 octave band averages)

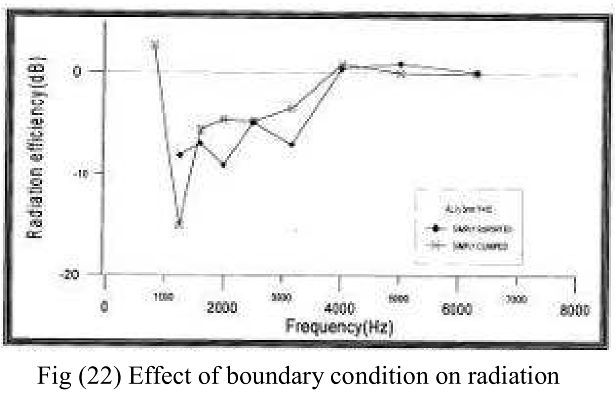

Fig (22) Effect of boundary condition on radiation efficiency of simply supported aluminum panel (1/3 octave band averages)

Table (1) Radiation efficiency of simply supported aluminum panel

Hz	Radiation efficiency (dB)															
	Y = 15 and thickness (mm) is				Y = 25 and thickness (mm) is				Y = 40 and thickness (mm) is				Y = 60 and thickness (mm) is			
	2	3	4	5	2	3	4	5	2	3	4	5	2	3	4	5
3100	-10.45	-7.47	1.57	0	-12.97	-8.86	-1.42	0	-14.41	-10.78	-3.14	-1.71	-16.57	12	-4.17	-3.61
4000	-10.63	0.52	2	-4.19	-12.43	-1.91	-1.14	-5.52	-14.59	-4.52	-3.28	-8	-16.39	-9.73	-5.42	-9.52
5000	-9.19	1.04	0	-1.90	-11.53	-1.73	-2.28	-4.19	-13.51	-3.82	-4.85	-5.71	-15.13	-6.08	-6.71	-7.80
6300	0	0	0	0	-1.26	-1.04	-0.85	-1.33	-3.65	-3.13	-3.85	-4.38	-5.40	-5.04	-5.42	-6.28

	Radiation efficiency (dB)															
	Y = 15 and thickness (mm) is				Y = 25 and thickness (mm) is				Y = 40 and thickness (mm) is				Y = 60 and thickness (mm) is			
	Y = 15 and thickness (mm) is				Y = 25 and thickness (mm) is				Y = 40 and thickness (mm) is				Y = 60 and thickness (mm) is			
	2	3	4	5	2	3	4	5	2	3	4	5	2	3	4	5
3100	-9.35	0.19	1.02	-2.09	-1.73	-7.45	-0.11	-2.58	-4.15	-12.74	-3.08	-4.19	-16.27	-14.11	-4.70	-4.35
4000	-10.38	-2.94	1.02	2.90	-3.98	-6.66	-2.05	-2.90	-5.88	-12.35	-4.11	-4.83	-15.41	-13.72	-6,17	-6.77
5000	-6.23	-3.13	-1.47	-6.77	-5.36	-7.84	-2.50	-9.57	-7.27	-9.41	-6.17	-10.96	-10.73	-8.62	-11.76	-12.90
6300	0	0	0	-0.32	-3.63	-3.52	-1.47	-1.12	-4.15	-5.21	-5.88	-3.87	-6.06	-7.84	-6.61	-5.16

Table (2) Radiation efficiency of simply supported glass panel

Table (3) Effect of boundary condition on radiation efficiency

Hz	Radiation efficiency (dB) for 3 mm panel thickness and Y = 15			
	Aluminum panel		Glass panel	
	Simply supported	Simply clamped	Simply supported	Simply clamped
3100	-7.47	-3.69	0.19	-5.88
4000	0.52	0.84	-2.94	2.74
5000	1.04	0	-3.13	-1.56
6300	0	0	0	0

Conclusions

The problem that we set out to solve was that of investigating the case of coupling between structures and acoustic spaces where the latter is driven by a noise source. We sought an approach that would be easy to understand and explain. This approach is based on using the result of coupled oscillatory theory between structural mode and acoustical modes. From the results obtained the following general concluding remarks are recorded:

(1) The radiation efficiency, which represents a measure for the structural response, decreasing as the damping increases. That was due to the increased power dissipated in both coupled sub-systems.
(2) Radiation efficiency increased as the thickness of the structural sub-system (panel) increases. This due to the dependence of the panel mode density on the thickness. As the thickness increases more structural modes are activated in the frequency band of interest and hence more available mode pairs.
(3) The radiation efficiency for a simply supported – clamped panel is higher than that for simply – simply supported panel.
(4) Generally, the response estimates get more reliable as the center frequency of the 1/3 octave band increases because of the increased number of acoustic – structural mode pairs. It is confirmed that the estimated radiation efficiency increases with frequency and approaches, asymptotically, that of the free filed value (σ = 0).

List of symbols

a & b	Panel dimensions in (m)
a, b & c	Box dimensions in (m)
B_{mr}	Acoustic-structural coupling factor
C	Speed of sound in (m/sec)
C_b	Flexural wave speed in (m/sec)
C_L	Longitudinal wave speed in (m/sec)
C_o	Speed of sound in the fluid in (m/sec)
D	Flexural rigidity of the panel in (N m)
E_{rad}	Radiation power in ($\frac{Nm}{\sec}$)
F_m & G_r	Generalized forces on mode m and mode r respectively in (N)
g_{mr}	Coupling constant
h	Thickness in (m)
k_p	Flexural wave number of the panel corresponding to the structural mode order m and n
k_r	Acoustic wave number corresponding to the acoustic mode order p, q and r
m & n	Structural modes
M	Total mass of the structure in (kg)
$m''(x)$	Mass density in (kg/m^3)
p, q & r	Acoustic mode order.
R_{rad}	Radiation resistance in (kg/sec)
Q	Quality factor
q'_r	Generalized coordinate of the acoustic velocity potential of the fluid in (m/sec)
S	Total area of the panel in (m^2)

S'_m	Generalized coordinate of the displacement of the structure normal to the surface in (m)
V	Volume of the space in (m^3)
x & r	Position vectors of points of structure and fluid respectively
β_m & β_r	Half power bandwidths of mode m and r respectively
ε_m & ε_r	Normalizing constant for the structural mode and acoustic mode respectively
η	Dissipation loss factor
η_m & η_r	Dissipation loss factors of the structure and acoustic modes respectively
θ'_m & θ'_r	Average, uncoupled, energies per unit mass of the oscillators subjected to input F'_m and G'_r in (N m/sec/kg)
ρ	Density of the fluid in the acoustic space in (kg/m^3)
ρ_o	Density of air in (kg/m^3)
ρ_s	Density of the panel in (kg/m^3)
$\phi_m(x)$	Displacement eigenfunction of structural mode m in (m)
$\psi_r(r)$	Velocity potential eigenfunction of acoustic mode r in (m/sec)
ω_m & ω_r	Natural frequencies of structural mode m and acoustic mode r respectively in (Hz)

References

1. Fahy F. J. and H. M. Ruivo, “Determination of statical energy analysis loss factors by means of an input power modulation technique” *Journal of sound and vibration*, 203 (5), pp 763-779, 1997.
2. James P. and F. J. Fahy, “A technique for the assessment of strength of coupling between SEA sub-system: Experiments with two coupled plates and two coupled room” *Journal of sound and vibration*, 203 (2), pp 265-282, 1997.
3. Frendi, L. Maestrello and L. Ting, “An efficient model for coupling structural vibration with acoustic radiation” *Journal of sound and vibration*, 182 (5), pp 741-757, 1995.
4. Shozo K., Atsushi M.and Takuzo I., “Study of active noise control by using structural acoustic coupled analysis” *The fifth international congress on sound and vibration*, South Australia, pp. 303-311, 1997.
5. Keiko Koshida, “The low frequency acoustic loading vibration response analysis of structures” *The fifth international congress on sound and vibration*, South Australia, pp 627-635, 1997.
6. Iglesis F. and Garcia F. P., “Dynamic behavior of a rectangular unbaffeld plate immersed in a diffuse field” *The fifth international congress on sound and vibration*, South Australia, pp 715-729, 1997.
7. Yan K. Tos and Ross G., “A study of the transmission of noise and vibration in an aluminum motor vessel” *The fifth international congress on sound and vibration*, South Australia, pp 2383-2391, 1997.
8. Kim S. and Brennan M., “A comparative study of feed forward control of harmonic and random sound transmission into an acoustic enclosure” *Journal of sound and vibration*, 226 (3), pp 549-571, 1999.
9. Guoyong J., Tiejun Y., Wanyou L. and Zhigang L. "Active control of sound transmission into an acoustic cavity surrounded by multiple flexible structural

boundaries" *The sixth international symposium on active noise and vibration control,* 2006.

10. Fahy F. J., "Vibration of containing structures by sound in the contained fluid" *Journal of sound and vibration*, 10 (3), pp 490-512, 1969.
11. Lyon R. and Maidanik G., "Power flow between linearly coupled oscillators" *Journal of acoustical Soc. Am.*, Vol. 34, pp 623, 1962.
12. Lyon R. and Scharton D., "Power flow and energy shearing in random vibration" *Journal of acoustical Soc. Am.*, Vol. 34, No. 6, pp 1332, 1968.
13. Newland D., "Calculation of power flow between coupled oscillators" *Journal of sound and vibration*, Vol. 3, pp 262, 1966.
14. Blevins R., "*Formulas for natural frequency and mode shape*", Van Nostrand Reinhold Company, New York, 1979.
15. Leo L. Beranek, "*Acoustics*", 1986.
16. Artheur W. Leissa, "*Vibration of plates*", 1969.
17. Lyon R., "*Statical energy analysis of dynamical systems: Theory and applications*", Cambridgr Maimit press, 1975.
18. "*Master catalogue, Electronic instruments*", Bruel & Kjare, 1989.
19. Jens T. Broch, "*Mechanical vibration and shock measurements",* Bruel & Kjaer Company, Denmark, 1984.
20. White R. and Walker J., "*Noise and vibration*", Ellis Horwood Ltd, England, 1982